AD-A151 472 MICROWAVE EMISSION FROM RELATIVISTIC ELECTRON BEAMS(U) 1/1
MASSACHUSETTS INST OF TECH CAMBRIDGE RESEARCH LAB OF
ELECTRONICS G BEKEFI 27 NOV 84 AFOSR-TR-85-0236
UNCLASSIFIED AFOSR-84-0026 F/G 20/8 NL

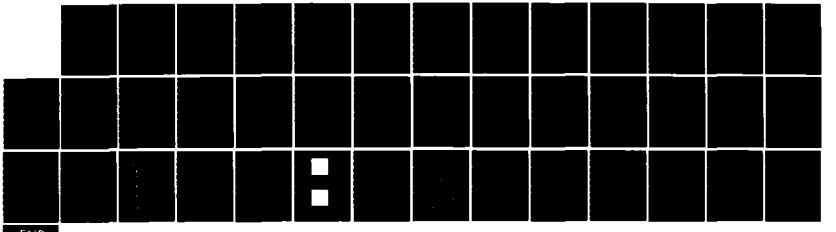

END
FILMED
DTIC

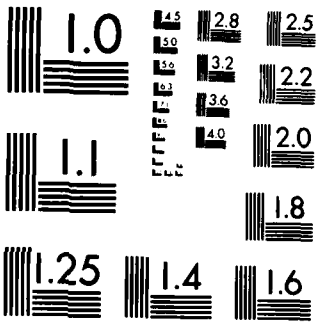

MICROCOPY RESOLUTION TEST CHART
NATIONAL BUREAU OF STANDARDS-1963-A

MASSACHUSETTS INSTITUTE OF TECHNOLOGY
RESEARCH LABORATORY OF ELECTRONICS
CAMBRIDGE, MASS. 02139

Interim Scientific Report on Grant AFOSR-84-0026

for research on

"Microwave Emission from Relativistic Electron Beams"

for the period

1 November 1983 - 31 October 1984

Submitted by

George Bekefi

November 27, 1984

UNCLASSIFIED

SECURITY CLASSIFICATION OF THIS PAGE

REPORT DOCUMENTATION PAGE

1a. REPORT SECURITY CLASSIFICATION: Unclassified	1b. RESTRICTIVE MARKINGS
2a. SECURITY CLASSIFICATION AUTHORITY	3. DISTRIBUTION/AVAILABILITY OF REPORT: Approved for public release; distribution unlimited
2b. DECLASSIFICATION/DOWNGRADING SCHEDULE	
4. PERFORMING ORGANIZATION REPORT NUMBER(S)	5. MONITORING ORGANIZATION REPORT NUMBER(S): AFOSR-TR- [illegible]
6a. NAME OF PERFORMING ORGANIZATION: Research Laboratory of Electronics, Massachusetts Institute of Technology (6b. OFFICE SYMBOL (If applicable))	7a. NAME OF MONITORING ORGANIZATION: AFOSR/NP
6c. ADDRESS (City, State and ZIP Code): 77 Massachusetts Avenue, Cambridge, MA 02139	7b. ADDRESS (City, State and ZIP Code): Bolling AFB D.C. 20332
8a. NAME OF FUNDING/SPONSORING ORGANIZATION: United States Air Force, Air Force Office of Scientific Research (8b. OFFICE SYMBOL (If applicable))	9. PROCUREMENT INSTRUMENT IDENTIFICATION NUMBER: AFOSR 84-0026
8c. ADDRESS (City, State and ZIP Code): Building 410, Bolling Air Force Base, D. C. 20332	10. SOURCE OF FUNDING NOS. — PROGRAM ELEMENT NO.: 61102F; PROJECT NO.: 2301; TASK NO.: A1; WORK UNIT NO.:
11. TITLE (Include Security Classification): Microwave Emission from Relativistic Electron Beams	
12. PERSONAL AUTHOR(S): George Bekefi	
13a. TYPE OF REPORT: Interim Scientific	13b. TIME COVERED: FROM 11/1/83 TO 10/31/84
14. DATE OF REPORT (Yr., Mo., Day): November 1984	15. PAGE COUNT: 39
16. SUPPLEMENTARY NOTATION	

17. COSATI CODES			18. SUBJECT TERMS (Continue on reverse if necessary and identify by block number)
FIELD	GROUP	SUB. GR.	

19. ABSTRACT (Continue on reverse if necessary and identify by block number)

We describe experiments on microwave and millimeterwave emission from free electron laser systems. The design, construction, and testing of a high quality electrostatically focussed field emission gun for free electron laser applications has been concluded.

20. DISTRIBUTION/AVAILABILITY OF ABSTRACT: UNCLASSIFIED/UNLIMITED [X] SAME AS RPT. [ ] OTIC USERS [ ]	21. ABSTRACT SECURITY CLASSIFICATION: Unclassified
22a. NAME OF RESPONSIBLE INDIVIDUAL: ~~Kyra M. Hall, RLE Contract Reports~~ Dr. Schlossberg	22b. TELEPHONE NUMBER (Include Area Code): 202/767-4906 — 22c. OFFICE SYMBOL: NP

DD FORM 1473, 83 APR — EDITION OF 1 JAN 73 IS OBSOLETE.

UNCLASSIFIED

SECURITY CLASSIFICATION OF THIS PAGE

SUMMARY OF EXPERIMENTAL RESEARCH ON GENERATION OF COHERENT RADIATION

In this section, we summarize recent experimental studies in the area of coherent radiation generation with free electron lasers.

a. A Submillimeter Raman Free Electron Laser Using a High Quality Electron Beam.

A free electron laser experiment is currently underway in which a 1kA, 2.1MeV electron beam is excited by a helical wiggler field of 2cm periodicity to produce submillimeter radiation at wavelengths between 400 and 600μm, (see Appendix 1). This experiment will operate in the high gain Raman regime with a maximum calculated output power at saturation of approximately 50MW.

This free electron laser is unique in two respects. First, the electron beam will be transported through the wiggler with the aid of two short solenoidal focussing lenses. This system obviates the need for a strong uniform guiding magnetic field in the interaction region thereby insuring that the cyclotron maser instability is not excited. Second, this FEL employs a very high quality electron beam. The beam is produced in a multielectrode electron gun which uses a cold field emission cathode. The gun consists of a planar cathode and anode grid followed by four accelerating stages. The accelerating electrodes are shaped to provide electrostatic focussing by balancing the self-electric and magnetic fields of the beam.

The transverse emittance of the beam and its axial spread are used as indicators of beam quality. The emittance of the electron beam has been measured by aperturing the beam into an array of small beamlets and observing the spreading and divergence of the beamlets downstream of the aperture plate. The emittance has been found to be highly dependent on cathode material and surface finish and on the electric field strength at the cathode surface. Some measured values of beam emittance for different cathode materials are listed in Appendix 2. The lowest emittance has been obtained with a soft graphite cathode and is found to decrease with increasing surface field strength. Under optimum conditions the measured normalized emittance ε_n is less than 50mrad-cm. The corresponding beam brightness, defined as $B=I/\pi^2\varepsilon_n^2$ where I is the beam current, is approximately $75kA/(rad\text{-}cm)^2$. This represents an order of magnitude increase in brightness over that achieved by other experimenters using nonimmersed field emission guns and is comparable to brightnesses achieved in guns requiring

that the cathode be immersed in very strong magnetic fields. The axial momentum spread in the beam is measured with a magnetic spectrometer of the Browne-Buechner type. Time resolved measurements show that the instantaneous axial momentum spread is less than 1%.

The magnetic wiggler for this free electron laser is currently under construction. We anticipate that radiation measurements will begin in January of 1985.

b. Low Voltage Free Electron Laser (Ubitron) Experiments.

A free electron laser is now operating in which a 35KeV electron beam propagates in combined linear wiggler and uniform axial magnetic fields. This experiment is designed to amplify microwave radiation at frequencies ranging from 4 to 8GHz with high efficiency. Details of the experimental arrangement may be found in Appendix 3.

The linear wiggler field is produced by a set of samarium cobalt permanent magnets. It has a periodicity of 2.0cm and an amplitude variable between 0.1 and 1.0kG. We have successfully propagated the electron beam through the wiggler, showing that the $\vec{B}\times\nabla\vec{B}$ drift of the electrons is sufficiently small for most values of the axial magnetic field to allow the beam to traverse the full length of the system. Also, the ability to tune the output frequency between 4.3 and 6.3GHz by varying the energy of the beam electrons has been demonstrated. The tuning curve is shown in Appendix 4.

We are currently in the process of increasing the beam current by a factor of 100 in order to increase the radiation gain.

c. Rippled Field Magnetron.

The rippled field magnetron is a novel cross-field generator of coherent radiation. It comprises a smooth cylindrical cathode enclosing a smooth cylindrical anode. Electrons emitted into the anode-cathode gap are subjected to both a uniform axial magnetic field and an azimuthally periodic radial wiggler magnetic field. Previous experiments have shown that this device radiates in a narrow spectral line in the frequency range 30-50GHz.

A new theoretical model of the rippled field magnetron has been developed. Details of this theory may be found in Appendix 5. This theoretical model predicts the linear increase of radiated frequency with axial magnetic

field observed in the experiment. Additional measurements are currently underway.

A1

APPENDIX 1

APPENDIX 1

A SUBMILLIMETER FREE ELECTRON LASER USING A HIGH QUALITY ELECTRON BEAM* D.A. KIRKPATRICK, R.E. SHEFER, and G. BEKEFI, MIT

A Raman free electron laser experiment to produce submillimeter wave radiation is in progress. The measured parameters of the electron beam are

Beam Voltage	1.6 MV
Beam Current Density	200 A-cm^{-2}
Axial Momentum Spread	$\leq$ 1%

Other experimental parameters are as follows:

Wiggler Period	2.0 cm
Number of Periods	50
Wiggler Field Amplitude	1200 Gauss
Output Frequency	456 GHz
Theoretical Single Pass Gain	23 dB
Saturated Efficiency	0.75%

The MIT Pulserad 110A accelerator facility is used in conjunction with a five stage electrostatically focused field emission electron gun to produce a high quality intense relativistic electron beam. The beam is then guided into a bifilar helical wiggler field by means of a short solenoidal coil which acts as a focusing lens. The coil is positioned upstream of the wiggler and obviates the necessity of having a guiding magnetic field in the wiggler region. The lack of a guide field in the wiggler region eliminates the possibility of exciting the cyclotron maser instability.

The beam quality has been determined by measurements of beam emittance and beam momentum spread.[1] Emittance measurements were carried out by allowing the beam to impinge on an array of pinholes in a brass disk, and then observing the transmitted beamlets on a flourescent screen at a known distance downstream. We find that the normalized emittance is $\leq$ 50 mr-cm. Beam momentum spread measurements were carried out using a magnetic spectrometer. Both time integrated and time resolved measurements show an axial momentum spread of less than one percent.

*This work is supported in part by the National Science Foundation, in part by the U.S. Air Force Office of Scientific Research and in part by the Department of the Air Force Aeronautical Systems Division (AFSC).

[1]R.E. Shefer, D.A. Kirkpatrick and G. Bekefi, Bull. Am. Phys. Soc. 28, 1063 (1983)

High Power Microwave and Submillimeter Wave Generation. 18

X

Douglas A. Kirkpatrick
Room 36-213
M.I.T.
Cambridge, MA. 02139

617 253-8533

A P P E N D I X 2

APPENDIX 2

HIGH BRIGHTNESS ELECTROSTATICALLY FOCUSSED FIELD EMISSION ELECTRON GUN FOR FREE ELECTRON LASER APPLICATIONS

D.A. Kirkpatrick, R.E. Shefer and G. Bekefi

Department of Physics and Research Laboratory of Electronics

Massachusetts Institute of Technology

Cambridge Massachusetts 02139

ABSTRACT

An electrostatically focussed, multi-stage electron gun using a cold (field emission) cathode has been developed for use in a free electron laser. This gun produces a 1.1 kA, 2.0 MV electron beam with a normalized emittance $\epsilon_n \simeq 38 \times 10^{-3}$ (π-cm-rad), and a brightness of 74 kA/cm^{2}rad^2. The measured brightness is almost two orders of magnitude higher than that found in most RF linacs, and is comparable to that achieved using electron guns immersed in strong guiding magnetic fields. The emittance and brightness have been studied as a function of cathode material, surface finish and the electric field strength at the cathode surface.

I. INTRODUCTION

Relativistic electron beams with high current densities and low temperatures are a prerequisite for the successful operation of free electron lasers[1](FEL's) and other sources of coherent radiation employing electron beams. If high radiation powers are also a requirement, high currents in addition to high current densities are necessary. These requirements[2] become more and more stringent the shorter the radiation wavelength.

Beam brightness[3] is a useful measure of beam quality. Previous experimental studies[4-7] and numerical simulations[8] have shown that electron guns with cold (field emission) cathodes can attain high brightness. Unfortunately, these guns had to be immersed in strong guiding magnetic fields ranging from 10 kG to 90 kG. Moreover, as much as 90% of the "hot" outer regions of the beam had to be scraped off thereby dramatically reducing the overall FEL efficiency.

In this paper we will show that high beam brightness can be achieved from a cold cathode field emission gun in the complete absence of a guiding magnetic field. We shall describe the operation of an electrostatically focussed, multi-stage field emission electron gun[9] which produces a 1.1 kA, 2.0 MV electron beam with a normalized emittance $\epsilon_n \simeq 38 \cdot 10^{-3}$ (π-cm-rad) and a brightness of 74 kA/cm^{2}rad^2. Its characteristics are comparable to or exceed those achieved by other experimenters using electron guns immersed in strong guiding magnetic fields. The gun consists of a planar cathode and anode grid, followed by four accelerating stages. The accelerating electrodes are shaped[10] to provide electrostatic

focussing and obviate the need for any external magnetic field in the gun region. With several accelerating electrodes rather than just one, the electric field strength at the cathode surface can be reduced sufficiently in order to minimize electron emission from unwanted surfaces(see below). Such extraneous emission spoils the beam quality.

In section II we describe our electron gun and the experimental arrangement used in measuring the beam current, beam profile, and beam emittance. In section III we discuss the results and in section IV we compare our observations with those of other workers.

II. EXPERIMENTAL ARRANGEMENT

The experimental setup is shown in Fig. 1. A Physics International Pulserad 110 A electron accelerator (0.6 – 2.5 MV, 30 kA, 20 ns) is used to energize a five-stage multi-electrode field emission electron gun shown in Fig. 2. The electron beam is generated in the gap between the cathode and first anode (A1) by field emission from an emitting surface embedded in the cathode. The aperture of the first anode (A1) is covered with an 80% optically transmitting molybdenum mesh. The resultant beam is then accelerated to the full voltage by stages two through five. The aperture in the last anode (A5) is also covered with an 80% optically transmitting molybdenum mesh.

The cathode plate is a spin-formed aluminum disk with a cylindrical hole in the center, allowing the insertion of a plug of emitting material. The entire surface of the cathode, with the exception of the small emitting area, is anodized to minimize undesired emission.

The hard aluminum oxide (anodized) coating has a thickness of 0.05 mm. The cathode is mounted on a stalk which is adjustable in the axial direction allowing us to vary the cathode to first anode gap spacing. Different emitting materials are studied by removing and changing the plug of emitting material.

The voltages on the successive anodes A1 to A4 are $[-\frac{3}{4}V_0, -\frac{1}{2}V_0, -\frac{1}{4}V_0, -\frac{1}{8}V_0]$, where V_0 is the full accelerator voltage. For a 2 MV beam, for example, the successive voltages in megavolts from the cathode to the last anode are $[-2, -1.5, -1.0, -0.5, -0.25, 0]$. This division is achieved by means of an axisymmetric, cylindrical copper sulfate voltage divider (see Fig. 2) with which the electrodes are in electrical contact. Typically, the total resistance of this divider equals 400Ω. The shapes of the electrodes are designed[10] with the view of balancing the self electric and self magnetic fields of the beam so as to produce a paraxial electron beam of radius $r \simeq 2.5$ cm.

A calibrated Rogowski coil mounted at the beam exit is used to measure the transmitted electron current. The beam voltage is obtained by means of a voltage divider placed between the fourth and last(grounded) anodes. Typical voltage and current pulse traces are shown in Fig. 3. The current density profile $J(r)$, which is required in determining the beam emittance, is measured by placing a series of concentric circular apertures after the mesh in the last anode, and observing the transmitted current as measured by the Rogowski coil at the beam exit as a function of aperture radius.

The emittance is measured[3,11] by allowing the electron beam to impinge on an array

Figure Captions

Fig. 1. Experimental arrangement (upper) and detail of emittance diagnostic (lower).

Fig. 2. Longitudinal cross-section of five stage multi-electrode gun.

Fig. 3. Oscilloscope traces of voltage on the electron gun (upper) and beam current (lower). The peak values are V = 2.0 MV and I = 1.1 kA.

Fig. 4. Phase space contour plots for beams produced at (a) a smooth POCO graphite cathode and (b) a smooth reactor graphite cathode. In both cases we show the contours of constant phase space density which enclose 90% of the beam electrons.

Fig. 5. Beamlet images on the ZnS scintillator screen for beams produced at (a) a smooth POCO graphite cathode and (b) a smooth reactor graphite cathode. In both cases V = 2.0 MV, the K-A gap spacing is 1.2 cm and the cathode diameter is 2.0 cm.

Fig. 6. Effective emittance ϵ_n/r_K vs applied electric field E in the cathode-anode gap for two different cathode materials.

Fig. 7. Electron beam brightnesses and beam currents measured in other experiments compared with those measured in this experiment (MIT-B). The circles represent electron guns immersed in strong magnetic fields ($B > 1$ kG), and the triangles represent non-immersed guns. The listed experiments UCSB[14] and MIT-A[15] use thermionic

Table I.

Current and Emittance as a Function of Cathode Material

$V = 2.0\,MV$, $K - A$ gap $= 1.20\,cm$, $2\,cm$ diameter emitting surface.

Cathode Material	Current (Amps)	$\delta\theta$ (mrad)	Emittance $(\times 10^{-3}\,(\pi - cm - rad))$	Brightness $(kA/cm^2 rad^2)$
Smooth POCO Graphite	750	18	270	1.0
Epoxy Inlaid Grooved POCO Graphite	930	8.9	180	2.9
Sandblasted 2024 Al	1300	5.2	104	12
Grooved POCO Graphite	1490	5.5	110	13
Carbon Coated Sandblasted 2024 Al	1610	4.2	86	22
Smooth Reactor Graphite	1660	4.2	83	24

17. C.W. Roberson, Proc. of Soc. of Photo-Optical Intr. Eng., **453**, 320 (1983).

18. R.E. Shefer and G. Bekefi, Appl. Phys. Lett. **37**, 901 (1980).

19. Y.Y. Lau and D. Chernin, Phys. Rev. Lett. **52**, 1425 (1984), and references therein.

20. P. Sprangle and A.T. Drobot, IEEE Trans. Microwave Theory Tech. **25**, 528 (1977), and references therein.

21. R.C. Davidson, "Theory of Nonneutral Plasmas", (W.A. Benjamin), p.66-78 (1974).

22. V.K. Neil, Jason Technical Report JSR-79-10 (1979).

23. J.D. Lawson, "The Physics of Charged Particle Beams", (Oxford University Press), p.201 (1977).

24. The brightness plotted for the NRL(VEBA) beam is obtained from reference [4] using the emittance calculated from the average quoted value of $\beta_\perp$. The error bars reflect the upper and lower bounds on the brightness calculated from the quoted upper and lower bounds on $\beta_\perp$.

8. M.E. Jones and L.E. Thode, J. Appl. Phys. **51**. 5212 (1980); M.E. Jones, M.A. Mostrom, and L.E. Thode. J. Appl. Phys. **52**, 4942 (1981); M.A. Mostrom, M.E. Jones, and L.E. Thode, J. Appl. Phys. **52**, 1266 (1981).

9. J. Fink, H.B. Schilling, and V. Schumacher, J. Appl. Phys., **51**, 2995 (1980).

10. W. Dommaschk, Max-Plank-Institut Für Plasmaphysik, Garching bei München, **IPP 0/12**, (1973).

11. B. Kulke and R. Kihara, Lawrence Livermore Laboratory Preprint UCRL-82533 (1979); J.G. Kelly and L.P. Bradley, Sandia National Laboratory Report SC-RR-72 0058 (1972).

12. POCO graphite is manufactured by UNION-76 Inc. The graphite used in this experiment is specified as type AXF-5Q.

13. D.D. Hinshelwood. IEEE Trans. on Plasma Sc., **PS-11**, 188 (1983); and D.D. Hinshelwood. Ph.D. thesis. Department of Physics, Massachusetts Institute of Technology, 1984 (unpublished).

14. L. Elias and G. Ramian. U. Cal. at Santa Barbara Report QIFEL18/83 (1983).

15. J. Fajans. G. Bekefi. Y.Z. Yin, and B. Lax. Phys. Rev. Lett. **52**. 246 (1984).

16. J.A. Pasour, private communication.

REFERENCES

1. P.A. Sprangle, R.A. Smith, and V.L. Granatstein, in "Infrared and Submillimeter Waves", ed. K. Button,(New York: Academic Press, 1980), Vol. 1, p.279 and references therein.

2. T.J. Kwan and C.M. Snell, Phys. Fluids **26**, 835 (1983).

3. C. Lejeune, and J. Aubert, in "Applied Charged Particle Optics", ed. A. Septier, (Academic Press), Part A, p.159 - 259 (1980).

4. R.H. Jackson, S.H. Gold, R.K. Parker, H.P. Freund, P.C. Efthimion, V.L. Granatstein, M. Herndon, A.K. Kinkead and J.E. Kosakowski, IEEE J. *of* Quantum Electron., **QE-19**, 346, (1983).

5. M.L. Sloan and H.A. Davis, Phys. Fluids **25**, 2337 (1982).

6. G.J. Caporaso. W.A. Barletta, D.L. Birx, R.J. Briggs, Y.P. Chong, A.G. Cole, T.J. Fessenden. R.E. Hester, E.J. Lauer, V.K. Neil, A.C. Paul, D.S. Prono, and K.W. Struve. Proc. of the Fifth Int. Conf. on High-Power Particle Beams, p.427 (1983); T.J. Fessenden. Lawrence Livermore National Laboratory Report UCID-19839 (1983).

7. R.L. Sheffield, M.D. Montgomery, J.V. Parker, K.B. Riepe, and S. Singer, J. Appl. Phys., **53**, 5408 (1982).

ACKNOWLEDGEMENTS

This work is supported in part by the Air Force Office of Scientific Research, in part by the National Science Foundation, and in part by the Lawrence Livermore National Laboratory. One of us (G.B.) also gratefully acknowledges help in gun design provided by Dr. H.B. Schilling.

through the relation,[22]

$$\frac{\Delta\gamma_{\|}}{\gamma} = \frac{\epsilon_n^2}{2r_b^2} \tag{3}$$

where r_b is the beam radius. For our best beam, the axial energy spread corresponding to the measured emittance at the exit of the electron gun, where $r_b = 2.5\,\mathrm{cm}$, is $\Delta\gamma_{\|}/\gamma = 1.2 \times 10^{-4}$.

The ultimate emittance $\epsilon_n(\mathrm{thermal})$ is one in which the electron temperature at the cathode surface T_K is the limiting parameter. Under these conditions,[23]

$$\epsilon_n(\mathrm{thermal}) \simeq 2r_K\left(\frac{\kappa T_K}{m_0c^2}\right)^{1/2} \tag{4}$$

where r_K is the cathode radius. Assuming that for a cold cathode the emitted electrons are in thermal equilibrium with the underlying plasma where the temperature is typically in the range[13] $3 - 10\,\mathrm{eV}$, one finds from Eq. (4) that $\epsilon_n(\mathrm{thermal}) \simeq (5-9) \times 10^{-3} r_K$ (π-cm-rad). For our 1 cm diameter cathode cited above, the corresponding beam brightness would be in the range $B_n(\mathrm{thermal}) \simeq (0.4 - 1.6) \times 10^4\,\mathrm{kA/cm^2 rad^2}$, which exceeds our best result by about two orders of magnitude.

One may also wish to compare the present result with the brightness obtained from the empirical Lawson-Penner condition often used to characterize beams produced by thermionic electron guns, namely,

$$\begin{aligned} \epsilon_n(L-P) &\simeq 0.3[I(\mathrm{kA})]^{1/2} \quad (\pi - \mathrm{cm} - \mathrm{rad}) \\ B_n(L-P) &\simeq 1.1 \quad \mathrm{kA/cm^2 rad^2} \end{aligned} \tag{5}$$

From this we see that the brightness of our beam is nearly two orders of magnitude greater than $B_n(L-P)$.

indicate that further increasing the surface electric field would most likely lead to even higher beam brightness. We note however that the maximum electric field that can be applied at the cathode is limited by the breakdown strength[9] of our anodized coating ($E \leq 900 - 1300\,\mathrm{kV/cm}$).

In Fig. 7 we plot our beam brightness along with those of beams produced in several other electron guns,[4-6,14-16] most of which find applications in free electron laser research. It has been suggested[17] that high brightness, high current electron beams can be achieved only through the use of guns immersed in strong magnetic fields ranging from approximately one kilogauss to tens of kilogauss. Figure 7 indicates that this is not necessarily the case, and that non-immersed guns can do as well (and possibly better) than immersed guns. This is a welcome conclusion. The reason for avoiding strong magnetic fields is threefold. First, strong magnetic fields occupying large volumes are often impractical. Secondly, magnetic fields cause a rippling of the beam surface. This has required experimenters[4,5,18] to remove as much as 90% of the hot outer layers, thereby reducing the overall efficiency of the free electron laser. Lastly, magnetic fields can give rise to undesirable instabilities, such as the negative mass instability,[19] the cyclotron maser instability,[20] and the diacotron instability.[21]

An important measure of beam quality[17] in a free electron laser is the fractional spread in beam axial energy $\Delta\gamma_{\|}/\gamma$, where $\gamma_{\|} = (1 - v_{\|}^2/c^2)^{-1/2}$. A finite transverse emittance corresponds to a spread in the transverse beam velocity and therefore to a spread in $\gamma_{\|}$

and to larger values of the rate of change of electric field dE/dt. There is evidence from other experiments[13] that increasing dE/dt results in improved cathode performance. We note that the 1 cm diameter smooth reactor graphite cathode at the 0.77 cm gap spacing produces the brightest beam, with a current of 1070 A, a normalized emittance of 38×10^{-3} (π−cm − rad), and a brightness of 74 kA/cm^{2}rad^2. The spreading angle $\delta\theta$ for the center beamlet for this case is 2.3 mrad. The phase space plot of the beam produced by this cathode is shown in Fig. 4(b).

The range of measurable emittances in this experiment is limited by the maximum acceptance angle of the aperture plate and by the minimum resolvable spot size on the film. The maximum acceptance angle is 460 mrad, which is almost an order of magnitude larger than the largest observed values of θ. The minimum resolvable $\delta\theta$ is approximately 2 mrad. Therefore, our lowest measured emittance of 38×10^{-3}(π−cm − rad) quoted above is resolution limited and represents an upper limit on the true emittance.

IV. CONCLUSIONS

We have studied the emittance characteristics of an electrostatically focussed, multistage, cold cathode electron gun. Measurements show that beam quality depends strongly on cathode material and on the strength of the applied electric field at the cathode surface. Our best results are obtained with a reactor grade graphite cathode with our highest applied electric field of 650 kV/cm. This configuration yields a normalized emittance of 38×10^{-3} (π-cm-rad) and a normalized brightness of 74 kA/cm^{2}rad^2. Our measurements

graphite cathode and the smooth reactor graphite cathode. The carbon coated sand-blasted 2024 aluminum cathode produces a beam with an emittance and a current very close to those of the beam from the smooth reactor graphite cathode. Finally, the last cathode consists of smooth POCO graphite with thin concentric ribbons of epoxy filling small grooves in the surface. This configuration yields low beam current and poor emittance.

Macroscopic Electric Field In the Cathode-Anode Gap.

Variation of the macroscopic electric field strength is achieved by varying the cathode-anode gap spacing from 0.77 cm to 2.05 cm. This results in a variation of the applied electric field strength from 650 kV/cm to 245 kV/cm, respectively. For the smallest gap spacing it is necessary to use a smaller cathode diameter because our 2 cm diameter cathodes emit an excessively large current which cannot be completely focussed by the electrode structure.

The observations are summarized in Fig. 6 where we plot an effective emittance ϵ_n/r_K, the normalized emittance divided by the cathode radius, as a function of the macroscopic electric field E in the K-A gap. By normalizing the emittance in this manner we remove the effects of different cathode radii. The quantity ϵ_n/r_K is a measure of $\delta\theta$ at the cathode. Figure 6 shows that lower effective emittances are obtained at higher macroscopic electric fields. This dependence is observed for both the grooved POCO graphite and smooth reactor graphite cathodes used in the experiment. These larger macroscopic electric fields correspond to larger local microscopic electric fields at the cathode surface,

to its greater porosity. When viewed with an electron microscope, this increased roughness extends to the microscopic scale; the graphite flakes in the POCO graphite are very ordered and lie flat on top of one another, while the graphite flakes in the reactor graphite are more randomly distributed and sharp protrusions are present. These protrusions and sharp edges on the microscopic scale produce a local electric field enhancement which may be responsible for the improved cathode turn-on and cathode plasma uniformity and therefore lower beam emittance. It is also possible that the reactor graphite has a significantly greater concentration of impurities. It has been suggested[13] that these impurities may also contribute to improved beam characteristics.

To measure the extent to which macroscopic protrusions affect emission and beam quality, concentric triangular grooves (0.5 mm deep, 0.75 mm radially separated) are cut into an otherwise smooth POCO graphite cathode. As can be seen from Table I, the result is a factor of two increase in observed current, and almost a factor of three decrease in measured emittance as compared to the smooth POCO graphite cathode. The improved beam characteristics obtained as a result of macroscopically roughening the POCO graphite cathode surface are still not as good as those obtained from a microscopically rough reactor graphite cathode.

Other cathode materials tested include sandblasted 2024 aluminum, sandblasted 2024 aluminum coated with carbon, and an epoxy inlaid POCO graphite cathode. Both the sandblasted 2024 aluminum and the carbon coated sandblasted 2024 aluminum cathodes produce beams with emittances which fall between those of the grooved POCO

ting surface 2 cm in diameter. A summary of these measurements is presented in Table I. In the first column is the current measured by the Rogowski coil when a mesh is in place in the last anode. In the second column is the spreading angle $\delta\theta$ of the center beamlet (see Fig. 1). Here $\delta\theta$ is the half-width-at-half-maximum of the intensity profile of the center spot on the photographic film. The third column gives the measured normalized emittance, calculated using the phase space area occupied by 90% of the beam electrons as outlined in section II. The last column is the brightness calculated from Eq. 2. The measured emittances listed in Table I range from the lowest value of 83×10^{-3} (π-cm-rad) for smooth reactor graphite to the highest value of 270×10^{-3} (π-cm-rad) for smooth POCO[12] graphite.

Two photographs of the beamlet images on the ZnS scintillator screen are shown in Fig. 5. Inspection of these photographs demonstrates the dramatic differences in the beams produced from these two cathode materials. For the case of the smooth POCO graphite, the spots are large, diffuse and irregular, and the emittance is correspondingly high. For the case of the smooth reactor graphite the spots are small, round and uniform, corresponding to a lower beam emittance.

The POCO graphite is a standard commercial graphite, which is relatively hard and dense($\rho = 1.84\,\mathrm{gm/cm^3}$). The reactor graphite is a softer graphite. which is more porous and less dense ($\rho = 1.66\,\mathrm{gm/cm^3}$) than the POCO graphite. The surfaces of both materials are faced off flat and are therefore macroscopically smooth. No attempt is made to polish either surface. On a smaller scale the surface of the reactor graphite cathode is rougher due

profile of the beam and a phase space contour plot is constructed. Two such contour plots are illustrated in Fig. 4, one for a poor emittance beam, the other for our best beam. Here $\theta_x = v_x/v_z$ is plotted against x, the transverse coordinate. Finally, the emittance ϵ_0 is defined[3] as $1/\pi$ times the area in x–θ_x space of the projection of the volume in phase space that encloses 90% of the beam electrons. The normalized emittance is then given by

$$\epsilon_n = \beta\gamma\epsilon_0 \tag{1}$$

where $\beta = v/c$, v is the beam velocity, and $\gamma = (1-\beta^2)^{-1/2}$ is the energy factor related to the accelerator voltage V_0 by $\gamma = 1 + (eV_0/m_0c^2)$. Once the emittance and beam current I are determined, the normalized beam brightness[3] can be calculated from

$$B_n = I/\pi^2\epsilon_n^2 \,. \tag{2}$$

III. RESULTS

The measured emittance and beam current are found to be functions of the cathode material and the electric field at the cathode surface. We present first the results of varying the cathode material, and second the results of varying the macroscopic electric field in the cathode-anode gap.

Cathode Material.

Emittance measurements are carried out with six different cathode materials at an accelerator voltage of 2.0 MV, a cathode-anode gap spacing of 1.2 cm, and a cathode emit-

of 25 pinhole apertures in a 1.0 mm thick tantalum disk which takes the place of the mesh in the last anode. The apertures, each 0.5 mm in diameter, are separated by a distance of 0.7 cm in a 5×5 square pattern.

The transmitted beamlets are then allowed to traverse a field free region 24.0 cm in length before they strike a thin (0.4 mm) aluminum target which is coated on the downstream side with ZnS scintillator (see Fig. 1). The illumination pattern is photographed via a large (20 cm $\times$ 20 cm) mirror by a 35mm camera. The camera is shielded with concrete blocks. These and the mirror allow us to photograph the scintillator screen during the shot, while keeping the film from being exposed by x-rays generated by electrons hitting the aperture plate and the aluminum target. The lens is stopped down to where the spots of light due to the beamlets striking the scintillator are just visible. This insures that the spots are in the "gray zone" of the film where its response is linear. The shutter of the camera is open for a period of time longer than the duration of the shot; therefore all emittance measurements are time integrated over one shot.

To evaluate the beam emittance, we first measure the intensity profiles of the individual beamlet images as recorded on the film. The image due to each beamlet is moved (in what we will call the x-direction) across a slit which is long (in the y-direction) and thin (in the x-direction). The length of the slit in the y-direction is, in all cases, larger than the extent of the image. In this way we effectively integrate over all velocities in one transverse dimension, while determining the velocity distribution in the other transverse dimension. This velocity distribution is then appropriately weighted by the measured current density

cathodes. The experiments ARA[5], ATA[6], NRL[16], NRL(VEBA)[24], and MIT-B use cold cathodes.

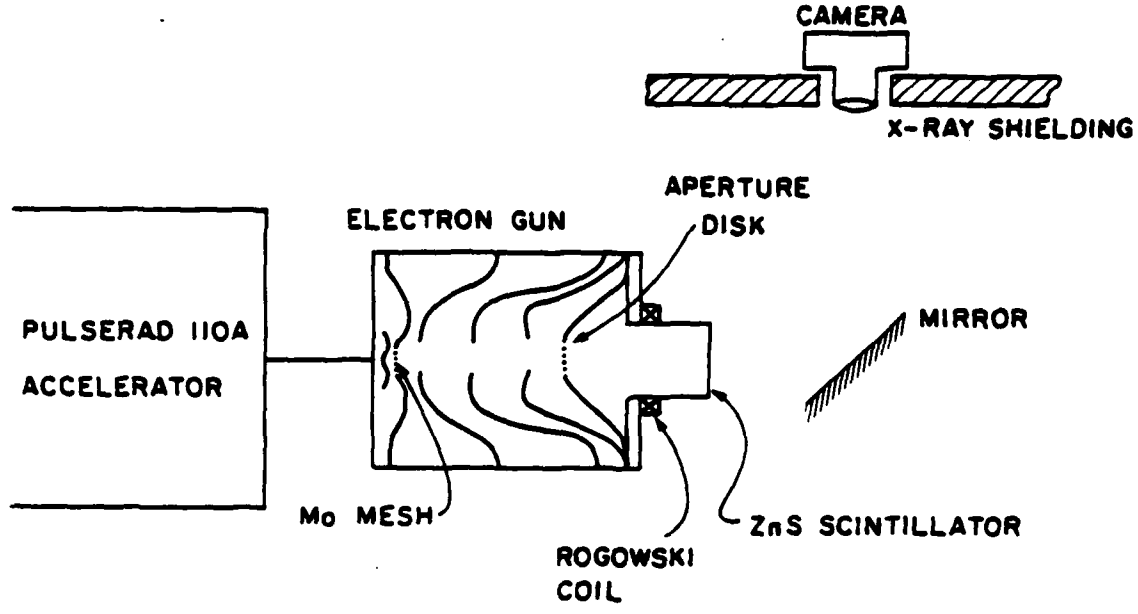

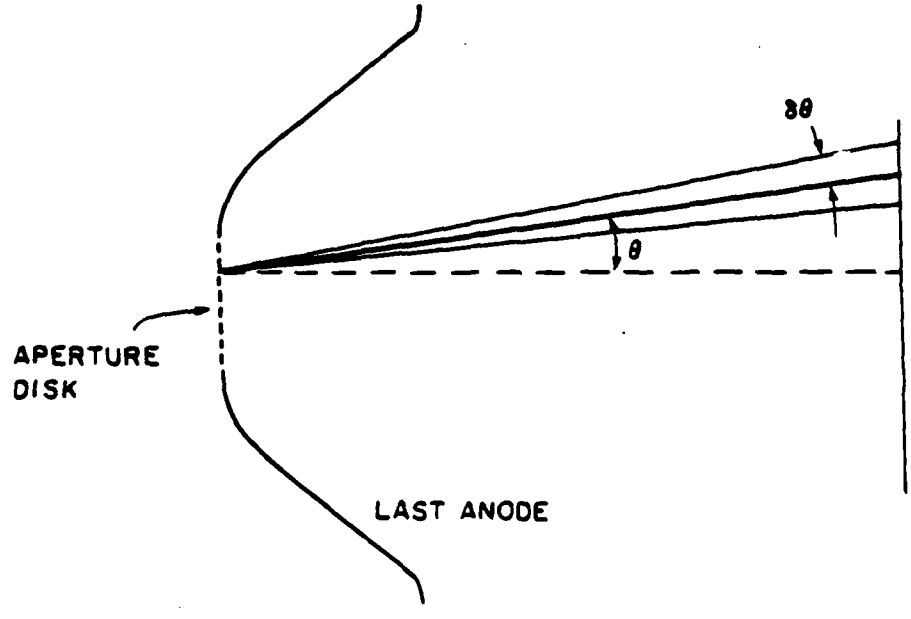

Fig. 1
Kirkpatrick, Shefer, Bekefi

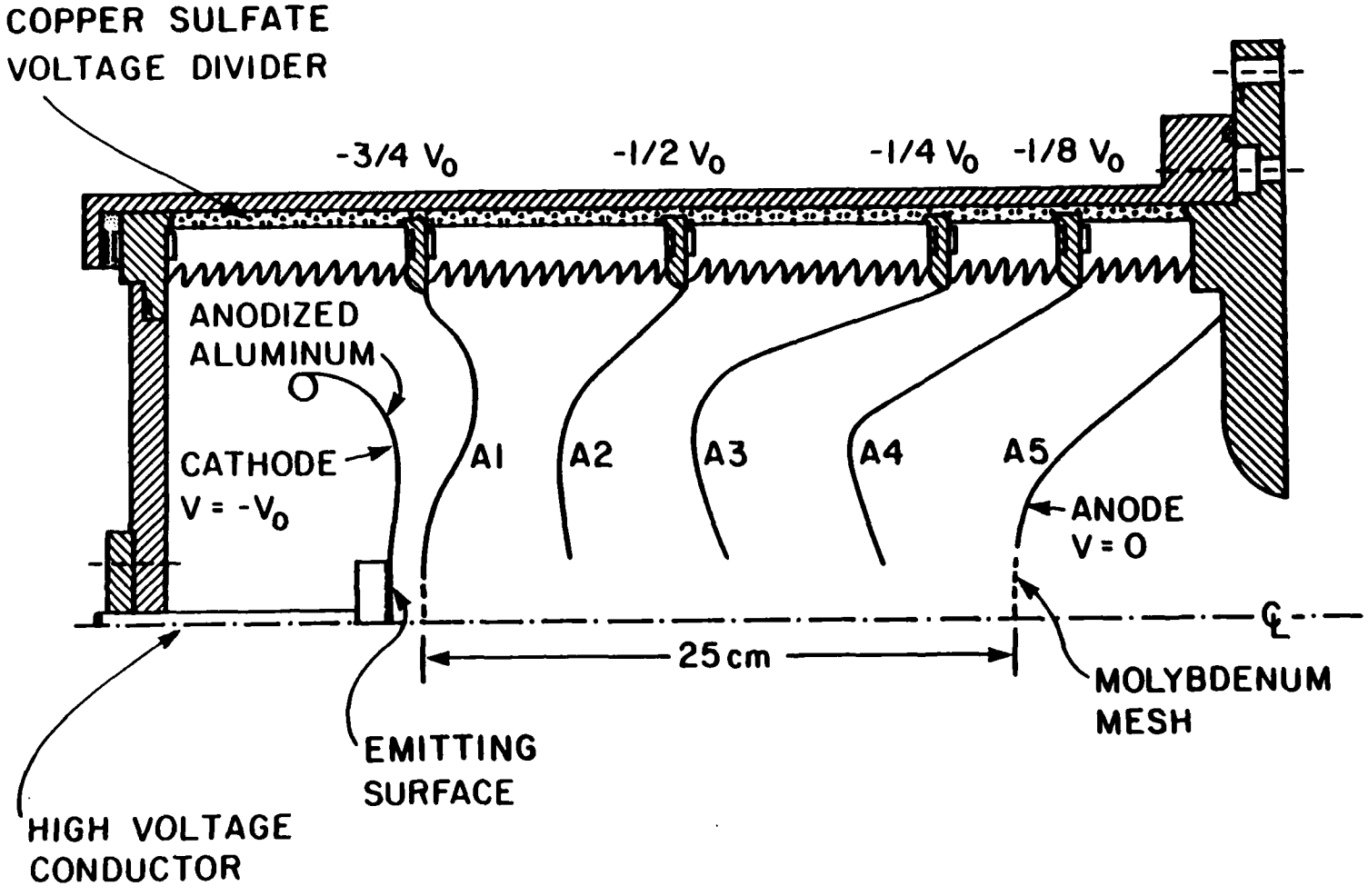

Fig. 2
Kirkpatrick, Shefer, Bekefi

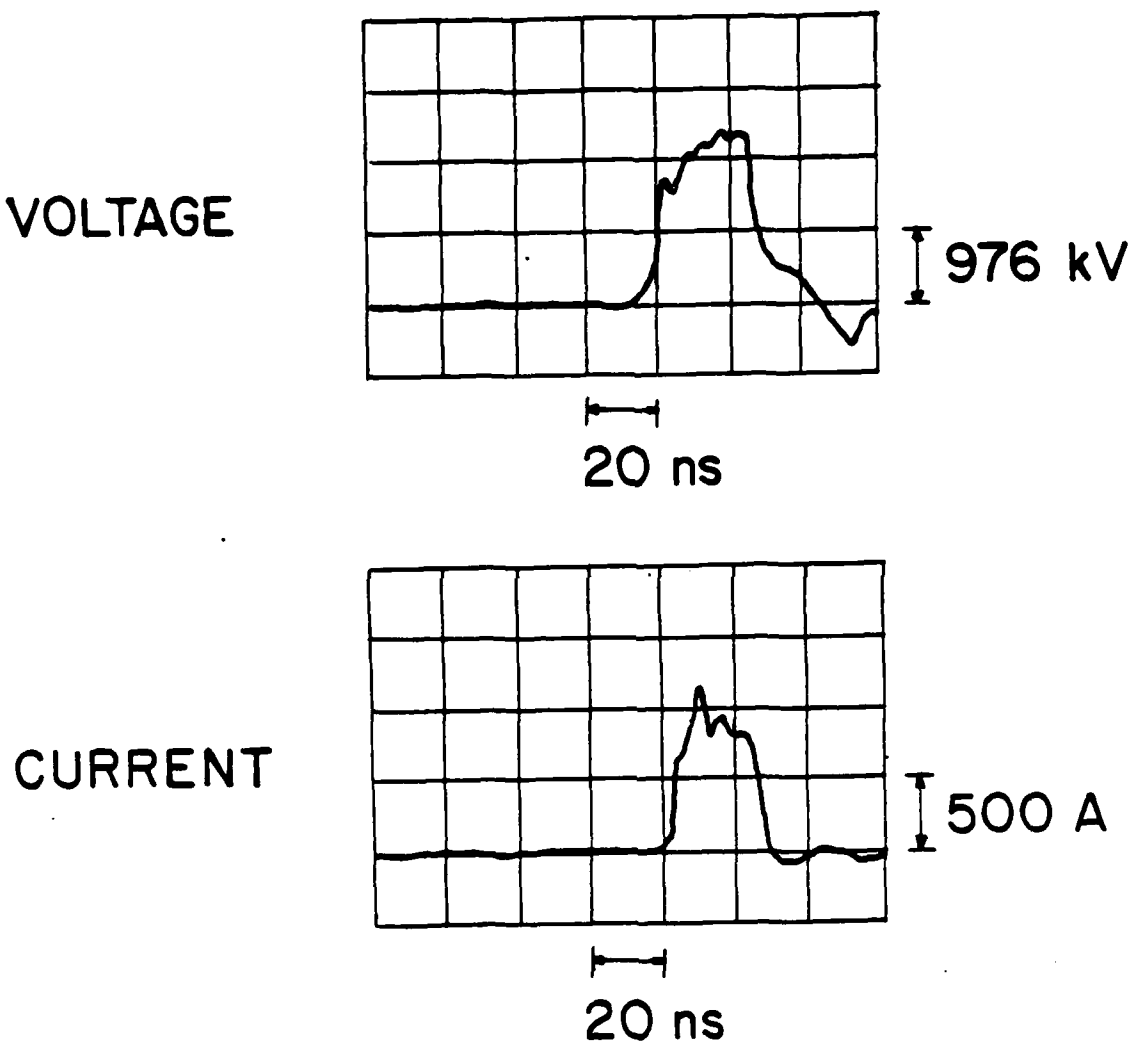

Fig. 3
Kirkpatrick, Shefer, Bekefi

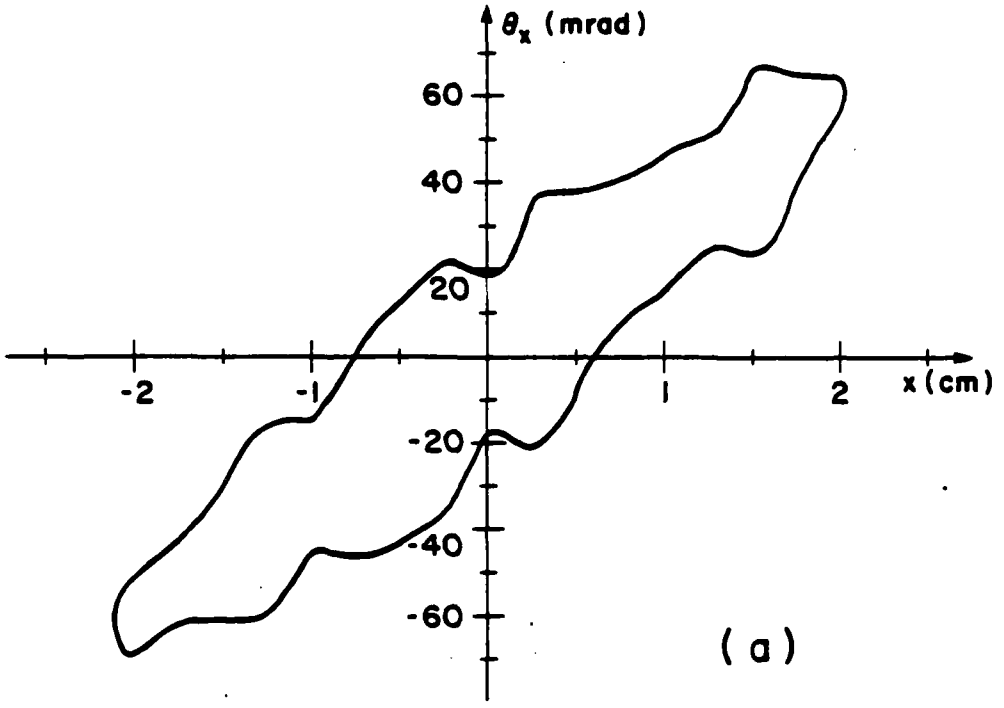

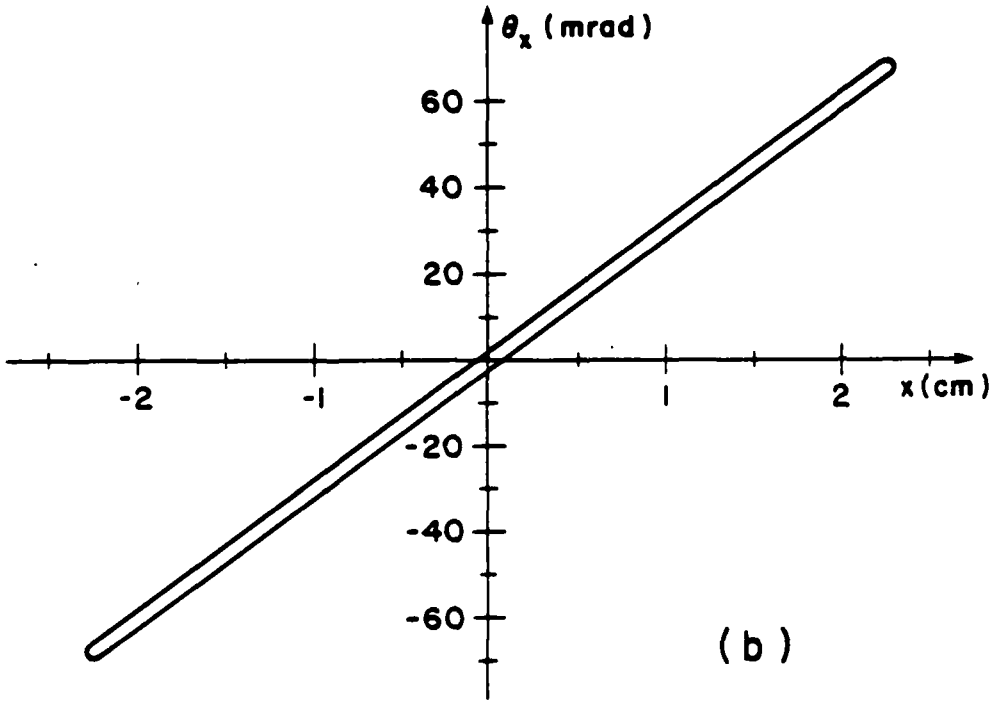

Fig. 4
Kirkpatrick, Shefer, Bekefi

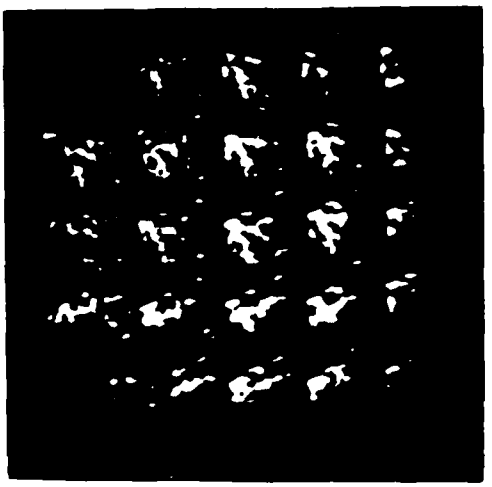

(a)

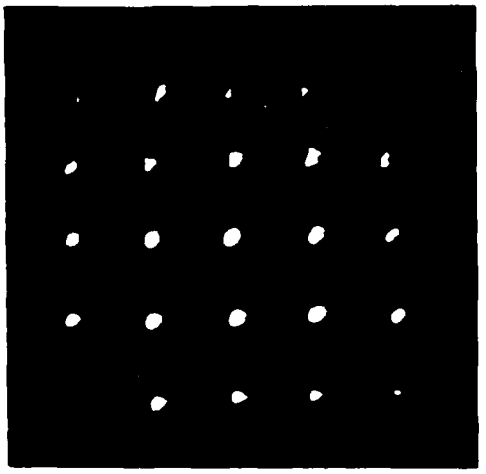

(b)

Fig. 5
Kirkpatrick, Shefer, Bekefi

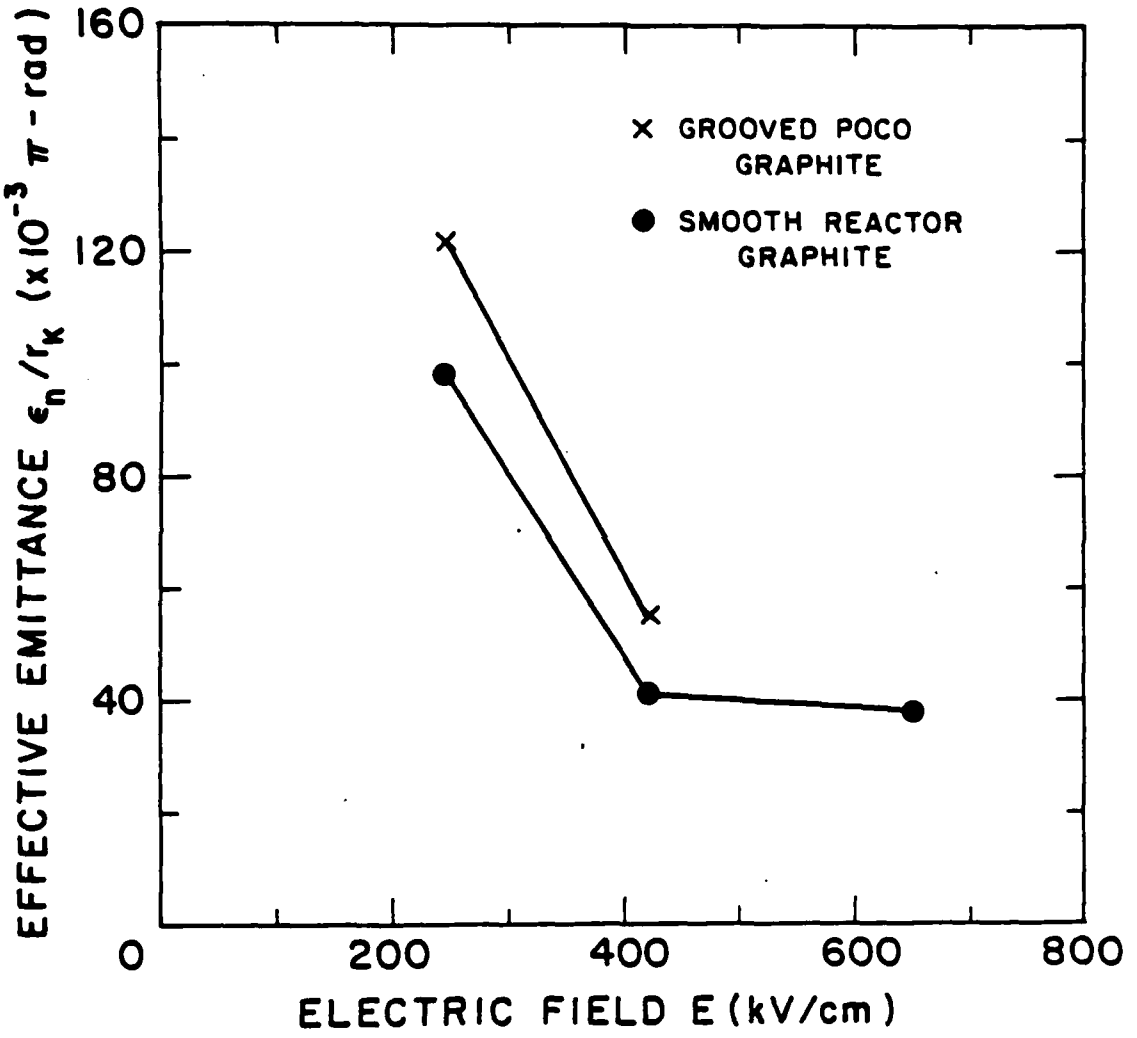

Fig. 6
Kirkpatrick, Shefer, Bekefi

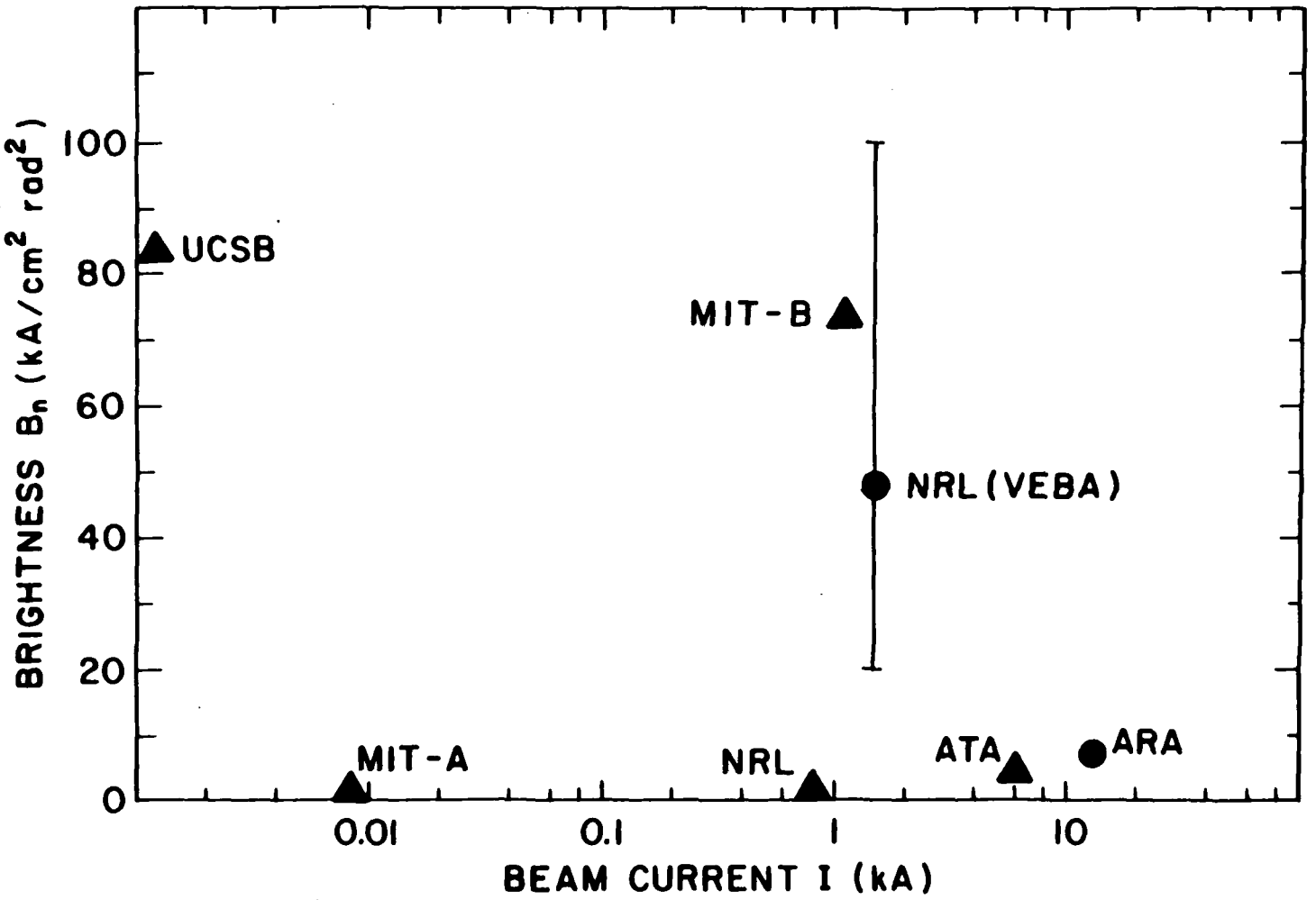

Fig. 7
Kirkpatrick, Shefer, Bekefi

APPENDIX 3

APPENDIX 3

Abstract Submitted for the

1984 IEEE INTERNATIONAL CONFERENCE ON PLASMA SCIENCE

May 14-16, 1984

Subject Category and number:
High Power Microwave and Submillimeter Wave Generation. 18

PREFER POSTER SESSION

Microwave Radiation and Electron Motion in a Ubitron with an Axial Guiding Magnetic Field.* K.D. JACOBS and G. BEKEFI, MIT--An experiment is underway to investigate the microwave and electron beam characteristics of a Free Electron Laser amplifier, similar to the Ubitron.[1] In this experiment, a 35keV, 1A electron beam is produced by a thermionic cathode. The beam pulsewidth is 1-5μsec, with a 0.001 duty cycle. A guiding axial magnetic field, generated by a series of D.C. powered, water cooled solenoid coils, is variable up to a maximum of B_0=3kG. This field both prevents radial expansion of the beam and allows investigation of the FEL gain near the resonance condition, $k_0 V_{\parallel} - \Omega_0/\gamma = 0$. ($k_0 = 2\pi/\ell$, ℓ=wiggler period, $\Omega_0 = (eB_0/m_0)$, $\gamma = (1-\beta^2)^{-\frac{1}{2}}$). A set of 480 samarium cobalt permanent magnets produces a linearly polarized wiggler magnetic field. The wiggler is 60 periods long, with periodicity ℓ=2.0cm, and entrance and exit tapers. The wiggler amplitude is variable from 0.1 to 1.0kG.

The beam drift tube is a length of WR-137 band rectangular waveguide. The 6GHz FEL output frequency lies in the lowest (TE_{10}) mode of the waveguide. A calibrated crystal detector and a conventional spectrum analyzer are used to make microwave power and frequency measurements. Determination of the electron beam axial velocity distribution is made using a gridded Faraday cup. Measurement of the beam properties and the microwaves can be made simultaneously.

The beam cross section has been observed with a fluorescent screen. It is found that the B×∇B drift of the beam is sufficiently small, for most values of the guide field, to permit propagation through the entire length of the system.

*This work was supported in part by the U.S. Air Force Office of Scientific Research, in part by the Department of the Air Force Aeronautical Systems Division (AFSC), and in part by the National Science Foundation.

[1]R.M. Phillips, IRE Transactions on Electron Devices ED-7, 231 (1960).

Submitted by:

Kenneth D. Jacobs

Kenneth D. Jacobs
Room 36-213
M.I.T.
Cambridge, MA. 01239
(617)253-5952

APPENDIX 4

APPENDIX 4

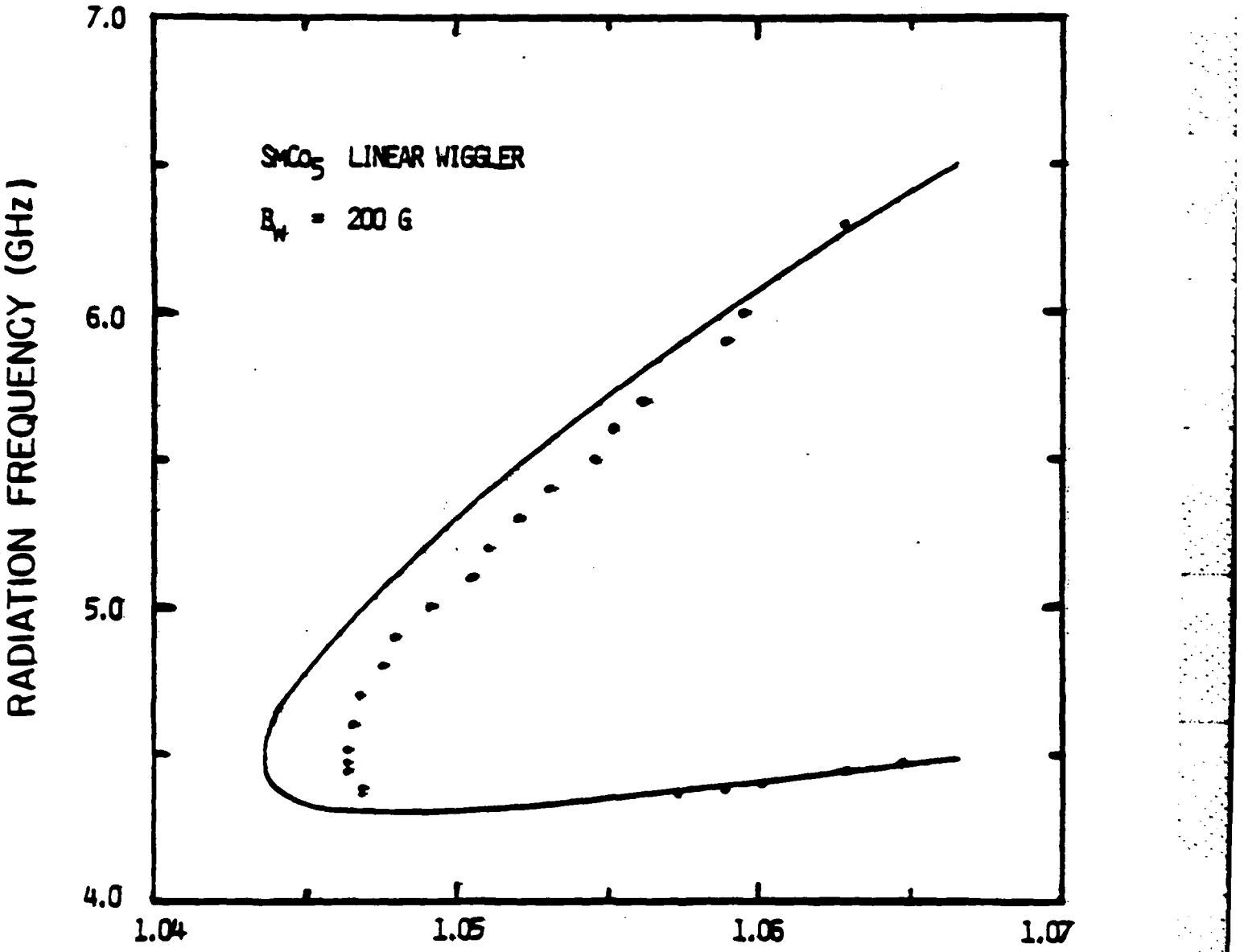

$$\gamma = 1 + \frac{eV}{m_0 c^2}$$

● Experiment

— Theory

APPENDIX 5

APPENDIX 5

Abstract Submitted for the

1984 IEEE INTERNATIONAL CONFERENCE ON PLASMA SCIENCE

May 14-16, 1984

Subject category and number:

High Power Microwave and Submillimeter Wave Generation. 18

PREFER POSTER SESSION

Submitted by:

Frederic Hartemann
Room 36-213
M.I.T.
Cambridge, MA. 02139
(617)253-2553

Theory and Simulation of the Rippled Field Magetron.* F.V. HARTEMANN, R.E. SHEFER, G. BEKEFI, MIT. nd A.T. DROBOT, SAI--A new theoretical model of the ippled field magnetron (RFM) has been developed. The redictions of this model are compared with the results f experiments carried out at MIT[1] and with a fully elativistic particle-in-cell simulation of the RFM.

The RFM comprises a smooth cylindrical cathode enlosing a smooth cylindrical anode. Electrons emitted rom the cathode are subject to both a uniform axial agnetic field $B_0\hat{z}$ and an azimuthally periodic radial iggler field of amplitude $B_w\hat{r}$ and wavenumber k_w. Experiments show that the RFM radiates in a single narrow pectral line ($\Delta f/f \leq 0.05$) whose frequency increases inearly with increasing B_0.

It is assumed that the system in the absence of ne wiggler is characterized by a Brillouin flow equilbrium in which the electrons undergo an azimuthal roation having sheared velocity $v_0(r)=E_0(r)/B_0\hat{\theta}$ where $_0(r)$ is the radial electric field in the gap. In the resence of a weak wiggler field ($B_w/B_0<<1$) we find nat in addition to the conventional first order undulatory motion along $B_0\hat{z}$ at frequency $k_w v_0(r)$ described y other researchers,[2,3] there exists a second order ndulatory motion transverse to $B_0\hat{z}$ at frequency $k_w v_0(r)$. This motion is due to the nonlinear coupling etween the undulations at $k_w v_0(r)$ and the wiggler field nd becomes very large for electrons whose radial position $r=r_0$ satisfies the resonant condition

$$2k_w v_0(r_0) = \frac{\Omega_0(r_0)}{\gamma_0(r_0)} . \qquad (1)$$

ere $\Omega_0(r_0)$ is the local relativistic cyclotron frequeny and $\gamma_0(r_0)=(1-v_0^2(r_0)/c^2)^{-1/2}$.

The dispersion relation for the RF fields produced y these resonant electrons exhibits growing modes whose requencies increase linearly with the applied uniform agnetic field B_0. This result is in agreement with xperimental observations, in contrast with previous neories[2,3] which predict a decrease in frequency with ncreasing B_0.

A computer simulation of the rippled field magnetron is being carried out using a fully relativistic, article-in-cell code (MASK). Electron trajectories nd spectra of the growing electromagnetic modes will be ompared with theoretical predictions and experimental bservations for a range of values of B_w and B_0.

Work supported in part by the U.S. Air Force Office of Scientific Research, in part by the Department of the Air Force Aeronautical Systems Division (AFSC), and in part by the National Science Foundation.

G. Bekefi, R.E. Shefer and B.D. Nevins, Proc. Int. Conf. on Lasers '82, ed. R.C. Powell, (STS Press, McLean, VA. 1982), p. 136.
R.C. Davidson, W.A. McMullin, and K. Tsang, Phys. Fliuds 27, 233 (1984).
C.L. Chang, E. Ott, T.M. Antonsen, Jr., and A.T. Drobot, SAI Report No. SAI-83-1214.

END

FILMED

4-85

DTIC